

# Asymptotic analysis of three-dimensional pressure interference tests: A line-injection line-monitoring solution

Walter A. Illman<sup>a,b</sup>, Daniel M. Tartakovsky<sup>c</sup>,

<sup>a</sup>*Department of Geoscience, University of Iowa, Iowa City, IA 52242*

<sup>b</sup>*Department of Civil & Environmental Engineering, and IIHR-Hydroscience & Engineering, University of Iowa, Iowa City, IA 52242*

<sup>c</sup>*Theoretical Division, Los Alamos National Laboratory, Los Alamos, NM 87545*

---

## Abstract

We present a new method to interpret three-dimensional pressure interference tests based on the asymptotic analysis of late time pressure transient data. The approach yields reliable estimates of equivalent permeability and porosity which can be obtained without the construction of type-curves or numerical inverse models. This is accomplished by developing an asymptotic solution for the line-injection line-monitoring solution derived by Hsieh and Neuman [1]. We apply our newly developed solution to a cross-hole pneumatic injection test data collected at the Apache Leap Research Site near Superior, Arizona [2] to obtain equivalent permeabilities and porosities. We find that permeabilities inferred from both the asymptotic and steady-state approaches [3] are similar. There is a weak correlation between the equivalent permeabilities and porosities and they both increase with the radial distance between the injection and monitoring intervals suggesting a scale effect in both parameters.

*Key words:* Permeability and porosity, pneumatic injection test, well test analysis, fracture flow, scale effect

---

## 1 Introduction

Various type-curve models developed for different hydrogeologic conditions allowed for the transient analysis of the time-drawdown data. For the technique

---

*Email addresses:* [walter-illman@uiowa.edu](mailto:walter-illman@uiowa.edu) (Walter A. Illman), [dmt@lanl.gov](mailto:dmt@lanl.gov) (Daniel M. Tartakovsky).

to be applicable and the parameter estimates to be meaningful, the time-drawdown data must fit the type-curves developed for the situation under consideration. In many cases these requirements are difficult to meet under field conditions due to factors that complicate the analysis. External factors such as recharge and barometric pressure fluctuations can corrupt the pressure transients making well test interpretation by means of traditional techniques difficult. Likewise, pressure transient data obtained from well tests conducted in heterogeneous media frequently do not match type-curves developed under the assumption that the medium is homogeneous. These complications limit the use of analytical type-curve approaches to simple situations. Numerical inverse approaches can overcome many of these difficulties by incorporating the effects of external forcings and heterogeneities, among other things, but these models can be complex and time-consuming to develop. Therefore, there is a need for alternative yet complementary interpretive approaches for the analysis of pressure interference tests to yield reliable estimates of flow parameters.

Illman and Tartakovsky [4] developed a new method to interpret three-dimensional pressure interference tests based on the asymptotic straight line analysis of late time pressure transient data. They applied their technique to several cross-hole pneumatic injection tests conducted at the Apache Leap Research Site near Superior, Arizona [2,5] to obtain equivalent permeabilities and porosities from these tests. These results were compared with previously obtained estimates of permeabilities and porosities from type-curve [6] and numerical inverse [7,8] analyses, as well as with permeabilities inferred from steady-state analysis [9]. The comparisons revealed that the newly developed approach yields reliable estimates of permeabilities and porosities from three-dimensional pressure interference tests.

They developed this method because of difficulties encountered in traditional well test interpretation approaches based on the analysis of steady-state or transient data. For the steady-state approach, the pressure transient data collected during a pressure interference test must reach a steady-state for the method to be applicable. These conditions in many cases are difficult to achieve because the pressure interference tests may have to be run for an exceedingly long time for steady-state conditions to develop. Even after running such a test for a long time, the pressure transients may never reach a steady state in some hydrogeologic conditions. In fact, well tests seldom reach a steady-state making the application of steady-state methods problematic. In addition, the steady-state analysis of pressure interference tests yields only the permeability but not estimates of porosity because of the reliance on the steady state portion of the data for the analysis. These are some important reasons why transient methods such as type-curve analysis, semi-log analysis [10], and numerical inverse modeling approaches have been developed to analyze the transient portion of the data.

The new approach developed by Illman and Tartakovsky [4] overcomes these difficulties and the approach yields reliable estimates of equivalent permeability and porosity which can be obtained without the construction of type-curves or numerical inverse models. However, the approximation presented in their paper is strictly valid for the case when the injection and monitoring intervals can be treated as points. In many field tests especially when the injection or monitoring interval is long and they are close to one another, this approximation is invalid. Therefore, solutions that consider the geometric relationship between the injection and monitoring intervals need to be developed to analyze three-dimensional pressure interference tests.

The objectives of this paper are to extend Illman and Tartakovsky [4]’s analysis by developing an asymptotic solution for the line-injection line-monitoring solution [1] and studying the late-time behavior. We then apply this approximation to one of the cross-hole pneumatic injection tests (labeled LL2) conducted at the Apache Leap Research Site near Superior, Arizona [2,5] to obtain equivalent permeabilities and porosities and compare these results to previously obtained estimates of permeabilities from steady-state analysis [3]. Finally, the correlation between the equivalent permeabilities and porosities are examined as well as their scale dependence.

## 2 Methodology

The methodology rests on obtaining a large time approximation to the line-injection line observation solution [1] originally developed for anisotropic aquifers. Here, we develop such an approximation to analyze three-dimensional pressure transient tests conducted using air as a flowing fluid in unsaturated geologic media. We note, however, that the approximation is also valid for the interpretation of pressure interference tests in saturated media.

The equations that describe airflow in partially saturated porous media are nonlinear due to the compressible nature of air, its capillary interaction with water, and non-Darcian behavior at high Reynolds numbers. A complete description of air-water interaction requires two systems of coupled partial differential equations, one for each phase. The development of corresponding analytical formulae [6] requires that two-phase flow is approximated as single-phase airflow and that water is treated as immobile. The airflow equation must additionally be linearized to allow solving it either in terms of pressure,  $p$ , as is customary for liquids or in terms of pressure-squared,  $p^2$ , as is more common for gases. Illman and Neuman [11] have shown that interpreting single-hole pneumatic injection tests at the ALRS by means of  $p^2$ -based and  $p$ -based type curves leads to similar results. Illman and Neuman [6] have shown that the

same holds true for cross-hole tests and therefore adopt the simpler  $p$ -based representation, as we do here.

The line-to-line solution is given by Eq. (35) in [1],

$$p_{dLL} = \frac{1}{4} \int_{1/(4t_d)}^{\infty} \frac{1}{w} \exp \left[ -(1 - \alpha_2^2)w \right] \int_{\lambda=-1}^1 \exp \left\{ - \left[ \lambda^2 \frac{1 - c^2}{\beta_1^2} + 2\lambda \frac{\beta_2 - \alpha_2 c}{\beta_1} \right] w \right\} \left\{ \operatorname{erf} \left[ \sqrt{w} \left( \alpha_2 + \frac{1}{\alpha_1} + \frac{\lambda c}{\beta_1} \right) \right] - \operatorname{erf} \left[ \sqrt{w} \left( \alpha_2 - \frac{1}{\alpha_1} + \frac{\lambda c}{\beta_1} \right) \right] \right\} d\lambda dw. \quad (1)$$

Here  $p_{dLL}$  is the dimensionless pressure defined for an isotropic medium as  $p_{dLL} = 4\pi kL\Delta\bar{p}/(q\mu)$ , where  $k$  is permeability,  $L$  is the length of the injection interval,  $\Delta\bar{p}$  is the average change in pressure in the monitoring interval,  $q$  is the flow rate, and  $\mu$  is dynamic viscosity. The dimensionless time is defined as  $t_d = kt p_{\text{ave}}/(\phi\mu r^2)$ , where  $p_{\text{ave}}$  is average pressure,  $\phi$  is porosity, and  $r$  is radial distance between the centroids of the injection and monitoring intervals.

The geometric relationships between the injection and monitoring intervals for the anisotropic case is described in [1]. For the isotropic case  $\alpha_1 = 2R/L$  where  $L$  is the length of the injection interval and  $\alpha_2 = \cos\theta_1$ , where  $\theta_1$  is the angle given in radians is between a unit vector pointing from the centroid of the injection interval toward the centroid of the monitoring interval and a unit vector parallel to the injection interval. Similarly,  $\beta_1 = 2R/B$  where  $B$  is the length of the observation interval and  $\beta_2 = \cos\theta_2$ , where  $\theta_2$  is the angle in radians between a unit vector pointing from the centroid of the injection interval toward the centroid of the monitoring interval and a unit vector parallel to the monitoring interval during the test. Note that  $c$  has a similar meaning as  $\alpha_2$  and  $\beta_2$  and is related to the angle between the injection and monitoring intervals.

We start our analysis of the asymptotic behavior of  $p_{dLL}$  at large time by evaluating the time derivative of (1),

$$\frac{dp_{dLL}}{dt_d} = \frac{1}{4t_d} \exp \left[ -\frac{1 - \alpha_2^2}{4t_d} \right] \int_{-1}^1 \exp \left\{ - \left[ \lambda^2 \frac{1 - c^2}{\beta_1^2} + 2\lambda \frac{\beta_2 - \alpha_2 c}{\beta_1} \right] \right\} \left\{ \operatorname{erf} \left[ \frac{\alpha_2 + 1/\alpha_1 + \lambda c/\beta_1}{2\sqrt{t_d}} \right] - \operatorname{erf} \left[ \frac{\alpha_2 - 1/\alpha_1 + \lambda c/\beta_1}{2\sqrt{t_d}} \right] \right\} d\lambda. \quad (2)$$

For large enough  $t_d$ ,

$$\exp \left[ -\frac{1 - \alpha_2^2}{4t_d} \right] \approx 1 - \frac{1 - \alpha_2^2}{4t_d}, \quad \operatorname{erf} \left[ \frac{A}{2\sqrt{t_d}} \right] \approx \frac{1}{\sqrt{\pi}} \frac{A}{\sqrt{t_d}}, \quad (3)$$

so that the leading term in the expansion of (2) is

$$\frac{dp_{dLL}}{dt_d} = \frac{\mathcal{I}}{4\alpha_1\sqrt{\pi}}t_d^{-3/2}, \quad (4)$$

where

$$\mathcal{I} = 2 \int_{-1}^1 \exp \left\{ - \left[ \lambda^2 \frac{1-c^2}{\beta_1^2} + 2\lambda \frac{\beta_2 - \alpha_2 c}{\beta_1} \right] \right\} d\lambda. \quad (5)$$

Evaluating (5) yields

$$\mathcal{I} = \frac{\beta_1}{\sqrt{1-c^2}} e^{A^2} \left[ \operatorname{erf} \left( A + \frac{\sqrt{1-c^2}}{\beta_1} \right) - \operatorname{erf} \left( A - \frac{\sqrt{1-c^2}}{\beta_1} \right) \right], \quad A = \frac{\beta_2 - \alpha_2 c}{\sqrt{1-c^2}}, \quad (6a)$$

for  $c \neq 1$ , and

$$\mathcal{I} = \frac{\beta_1}{\beta_2 - \alpha_2} \left[ \exp \left( 2 \frac{\beta_2 - \alpha_2}{\beta_1} \right) - \exp \left( -2 \frac{\beta_2 - \alpha_2}{\beta_1} \right) \right], \quad (6b)$$

for  $c = 1$ . It follows from (4) that the pressure derivative decays with time at the rate  $t_d^{-3/2}$ . This result is analogous to the result obtained by Illman and Tartakovsky [4] for a point-source solution.

Integrating (4) yields the asymptotic behavior of dimensionless pressure at large dimensional time

$$p_{dLL}(t_d) = p_{dLL}(t_d = \infty) - \frac{\mathcal{I}}{2\alpha_1} t_d^{-1/2}, \quad (7)$$

where  $p_{dLL}(\infty)$  is the steady-state solution. For  $c \neq 1$ , it is given by Eq. (54) of Hsieh and Neuman [1985],

$$p_{dLL}(\infty) = \frac{1}{2} \int_{-1}^1 \ln \left[ \frac{\left\{ \sqrt{\frac{\alpha_1^2 \lambda^2}{\beta_1^2} + 2\lambda \frac{\alpha_1^2 \beta_2 + \alpha_1 c}{\beta_1} + \alpha_1^2 + 2\alpha_1 \alpha_2 + 1} + \alpha_1 \alpha_2 + 1 + \frac{\alpha_1 c \lambda}{\beta_1} \right\}}{\left\{ \sqrt{\frac{\alpha_1^2 \lambda^2}{\beta_1^2} + 2\lambda \frac{\alpha_1^2 \beta_2 - \alpha_1 c}{\beta_1} + \alpha_1^2 - 2\alpha_1 \alpha_2 + 1} + \alpha_1 \alpha_2 - 1 + \frac{\alpha_1 c \lambda}{\beta_1} \right\}} \right] d\lambda. \quad (8)$$

It follows from (7) that the dimensionless pressure varies linearly with  $1/\sqrt{t_d}$  for large enough values of dimensionless time  $t_d$ . This finding coincides with that obtained by Illman and Tartakovsky [4] for the point-source solution.

Figure 1 compares the dimensionless pressure  $p_{dLL}$  computed with the solution of Hsieh and Neuman [1] (solid curves) and our asymptotic solution (dashed lines). For the purpose of data analysis, the two solutions are identical for

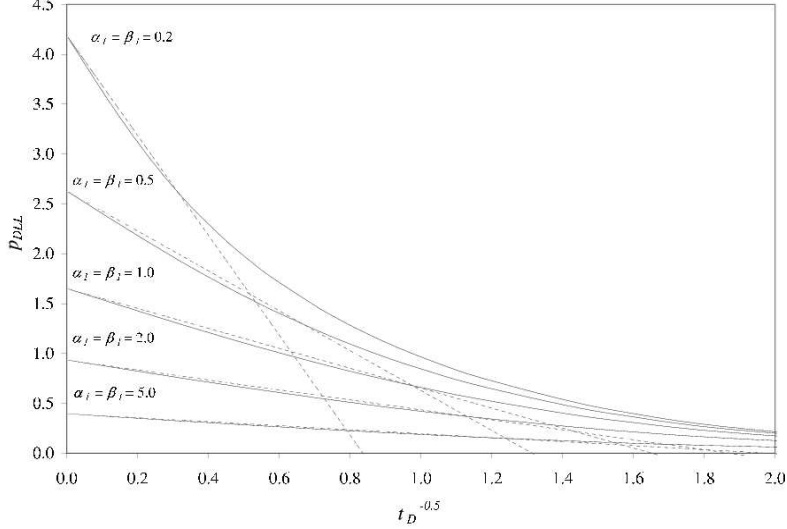


Fig. 1. Dimensionless pressure  $p_{dLL}$  computed with the solution of Hsieh and Neuman [1] (solid curves) and the asymptotic solution (7) (dashed lines).

intermediate to late dimensionless time (small  $1/\sqrt{t_d}$ ), with the correspondence improving as  $\alpha_1 = \beta_1$  increase. The approximation can be used to infer hydraulic parameters from line-to-line pumping tests when  $\alpha_1 = \beta_1 > 0.2$ . The accuracy of the asymptotic solution (7) depends on the accuracy of the approximations (3). This leads to the following constraints on the duration of a pumping test,

$$t_d \gg \frac{1 - \alpha_2^2}{4}, \quad t_d \gg \frac{(\alpha_2 \pm 1/\alpha_1 + \lambda c/\beta_1)^2}{4}. \quad (9)$$

These relationships provide useful guidelines for the design of pumping tests, when they are interpreted using our approach.

To infer the equivalent permeability and porosity from pressure data from the monitoring interval, we write (7) in its dimensional form as

$$\Delta \bar{p} = \frac{q\mu}{4\pi kL} p_{dLL}(\infty) - \left( \frac{q\mu r}{4\pi kL} \frac{\mathcal{I}}{2\alpha_1} \sqrt{\frac{\phi\mu}{kp_{ave}}} \right) t^{-1/2}. \quad (10)$$

Since  $\Delta \bar{p}$  varies linearly with  $t^{-1/2}$ , we plot the change in pressure,  $p$ , at a given monitoring interval against values of the reciprocal of the square root of time  $t^{-1/2}$ . A straight line should develop for a portion of the data to which a straight line is fit. Let  $\Delta \bar{p}^*$  denote the intersection of this straight line with the time axis  $t^{-1/2}$ . Then permeability  $k$  is determined from

$$k = \frac{q\mu}{4\pi L \Delta \bar{p}^*} p_{dLL}(\infty). \quad (11)$$

Similarly, let  $t^*$  denote the time at which the straight line crosses the horizontal

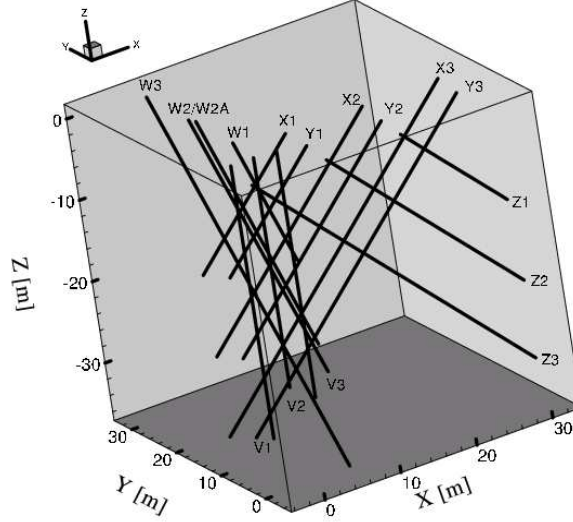


Fig. 2. Vertical and inclined boreholes within a geologically distinct unit of partially welded unsaturated tuff in the test site near Superior, Arizona.

coordinate, i.e.,  $\Delta\bar{p} = 0$ . Then porosity  $\phi$  is determined from

$$\phi = \frac{kp_{ave}t^*}{\mu r^2} \left( \frac{2\alpha_1}{\mathcal{I}} \right)^2 p_{dLL}^2(\infty). \quad (12)$$

This method of determining the permeability and porosity of porous formation is more accurate and less prone to interpretive errors than the currently used curve matching approach.

### 3 Application to three-dimensional pressure interference tests

We apply our technique to a three-dimensional pressure interference test with the line-injection/lin-observation configuration conducted at the Apache Leap Research Site (ALRS).

#### 3.1 Site and test description

The site is located near Superior, Arizona at an elevation of 1,200m above sea level. The test site included 22 vertical and inclined (at 45°) boreholes that have been completed to a maximum depth of 30m within a geologically distinct unit of partially welded unsaturated tuff. Figure 2 shows three-dimensional perspective view of the 16 of the 22 boreholes at the site. The upper 1.8 m of each borehole was cased. Core samples were taken from 9 of the 22 boreholes and a variety of tests were performed [12] to determine the interstitial properties of the tuff matrix. Single-hole pneumatic and hydraulic injection tests

were conducted with both an injection interval length of  $3m$  [12] and various injection interval lengths [13] to determine estimates of permeabilities of the fractured tuff. Additional details on these tests and the site can be found in [2].

Core and single-hole pneumatic injection tests provide information only about a small volume of rock in the close vicinity of the injection interval. Fractured rock properties measured on such small scales tend to vary rapidly and erratically in space so as to render the rock strongly and randomly heterogeneous. To determine the properties of the rock on larger scales, numerous cross-hole pneumatic injection tests were conducted [2,5] between 16 boreholes (one of which included all 22 boreholes), 11 of which have been previously subjected to single-hole testing. The tests consisted of injecting air into an isolated interval within one borehole while monitoring pressure responses in isolated intervals within this and all other boreholes. The purpose of these tests was to determine the bulk pneumatic properties of larger rock volumes between boreholes at the site, and the degree to which fractures are pneumatically interconnected.

The tests were performed using modular straddle packer systems that were easily adapted to various test configurations and allowed rapid replacement of failed components, modification of the number of packers, and adjustment of distances between them in both the injection and monitoring boreholes. The main injection string consisted of 3 packers, one near the soil surface to isolate the borehole from the atmosphere, and two to enclose the injection interval. The air-filled volume of the injection interval was made relatively small so as to minimize borehole storage effects. Intervals with a single packer near the soil surface (of which we had six) are identified below by borehole designation; for example V1, X1 and W1. Where a modular system separates a borehole into three isolated intervals, we append to the borehole designation a suffix U, M or B to identify the upper, middle or bottom interval, respectively; for example V3U, V3M and V3B. Where a modular system separates a borehole into four isolated intervals, we append to the borehole designation a suffix U, M, L or B to identify the upper, middle, lower or bottom interval, respectively; for example Z2U, Z2M, Z2L, and Z2B.

A typical cross-hole test consisted of packer inflation, a period of pressure recovery, air injection and another period of pressure recovery. Our system allowed rapid release of packer inflation pressure when the corresponding recovery was slow, but this feature was never activated even though recovery had sometimes taken several hours. Once packer inflation pressure had dissipated in all (monitoring and injection) intervals, air injection at a constant flow rate began. It generally continued for several days until pressure in most monitoring intervals appeared to have stabilized. In some tests, injection pressure was allowed to dissipate until ambient conditions have been recovered. In

Table 1

Geometric parameters of monitoring intervals during cross-hole test LL2

Interval	$R[m]$	$B[m]$	$\alpha_1$	$\alpha_2$	$\beta_1$	$\beta_2$	$c$
V2	2.19	24.25	0.35	1.04	0.39	0.67	0.71
V3	3.36	26.48	0.34	0.69	0.35	0.93	0.71
W1	8.08	11.35	0.48	0.85	1.09	0.63	0.50
W2A	5.10	26.14	0.35	0.20	0.36	0.74	0.50
X2	5.72	28.61	0.36	0.01	0.34	0.01	1.00
X3	9.18	42.64	0.64	0.02	0.40	0.03	1.00
Y1	7.97	13.19	0.53	0.15	1.09	0.07	1.00
Z2	18.17	27.50	1.19	0.66	1.17	0.67	0.00

other tests, air injection continued at incremental flow rates, each lasting until the corresponding pressure had stabilized, before the system was allowed to recover.

Three types of cross-hole tests were conducted at the ALRS in 3 phases. Phase 1 included line-injection/line-monitoring (LL) tests in which injection and monitoring took place along the entire length of a borehole that had been isolated from the atmosphere by means of shallow packers. Some of the boreholes were open to the atmosphere. Phase 2 consisted of point-injection/line-monitoring (PL) tests in which air was injected into a  $2 - m$  section in one borehole while pressure was recorded along the entire length of each monitoring borehole. During Phase 3, we conducted point-injection/point-monitoring (PP) tests in which both the injection and the monitoring intervals were short enough to be treated as points for purposes of type-curve analysis [6]. All of the boreholes were packed off during the PL and PP tests. A total of 44 cross-hole pneumatic interference tests of various types (constant injection rate, multiple step injection rates, instantaneous injection) have been conducted using various configurations of injection and monitoring intervals (LL, PL and PP).

### 3.2 Results

Recently, we applied our asymptotic approach to analyze data from various cross-hole pneumatic injection tests in unsaturated fractured tuff. The asymptotic analysis was conducted on tests deemed successful in that 1) they did not suffer from significant equipment failure and 2) their flow conditions were relatively well controlled and stable. Here, we analyze selected data from one such test LL2 which was previously subjected to steady-state analysis [3]. However, a type-curve or numerical inverse analysis has not been done using this test.

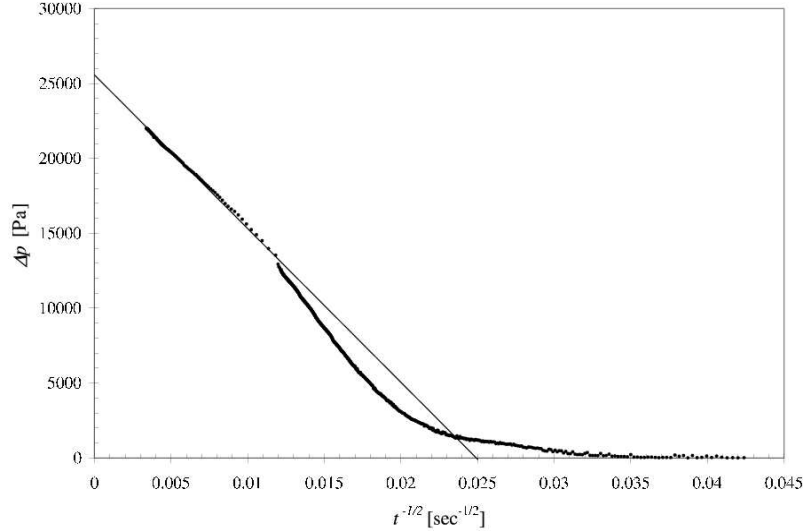


Fig. 3. Data from line monitoring interval V2 from cross-hole test LL2 and their asymptotic analysis.

We apply the asymptotic straight line approach to pressure data in which both the injection and monitoring intervals are treated for the purpose of analysis, as lines. There are two tests (LL1 and LL2) available for the interpretation but we choose LL2. LL1 was conducted with a volumetric flow rate ( $q$ ) of 50 standard liters per minute (SLPM) while LL2 was conducted at a higher flow rate of 100 SLPM thus yielding a stronger responses in a larger number of borehole intervals. Table 1 lists the name of the borehole intervals that were monitored during test LL2, their radial distance ( $R$ ) from the injection interval, their lengths ( $B$ ), and the geometric parameters described earlier.

Figure 3 shows the results from analyzing data from line monitoring interval V2 from cross-hole test LL2. Details to the test are given in [2]. It reveals that after an early time behavior that may be dominated by the effects of borehole storage, skin, and heterogeneity, a straight line develops. A visual examination of all pressure records examined reveals that all of them attain this straight line behavior at sufficiently large time and therefore is amenable to our asymptotic analysis. In many of the data that we examined, the signal to noise ratio was large making the definition of the straight line portion of the pressure transients relatively easy.

We also plot data obtained from line monitoring interval Z2 on Figure 4 and analyze it with our asymptotic straight line approach. It is evident from the figure that the signal-to-noise ratio is considerably lower making the analysis more difficult with traditional approaches such as with the type-curve approach. However, we see the development of a straight line at large times (small  $t_d^{-1/2}$ ) making the analysis possible with our approach.

Log<sub>10</sub>-transformed permeability values from the asymptotic analysis of 8 in-

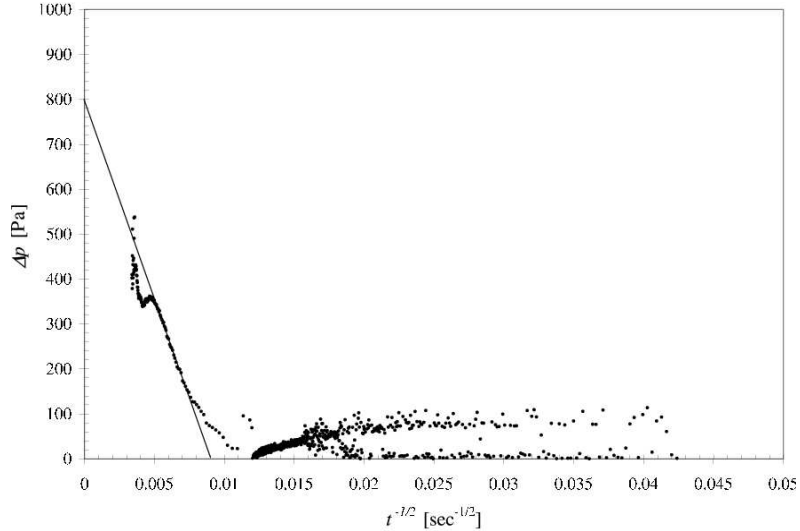


Fig. 4. Data from line monitoring interval Z2 from cross-hole test LL2 and their asymptotic analysis.

tervals range from  $-14.25$  ( $5.60 \times 10^{-15} m^2$ ) to  $-12.59$  ( $2.57 \times 10^{-13} m^2$ ) with the geometric mean of  $-13.60$  ( $2.49 \times 10^{-14} m^2$ ). Likewise, the  $\log_{10}$ -transformed porosity values range from  $-2.85$  ( $1.49 \times 10^{-3}$ ) to  $-0.59$  ( $2.59 \times 10^{-1}$ ) with the geometric mean of  $-1.48$  ( $3.24 \times 10^{-2}$ ). More meaningful statistical analysis of these data is not possible, since only 8 data points are available.

Our analysis of pressure transient data assumes that the rock is pneumatically uniform and isotropic on the scale of the cross-hole test. However, data from different monitoring intervals are seen to yield different values of pneumatic parameters, thereby providing information about their spatial and directional dependence. The values of permeabilities and porosities can be viewed as bulk directional properties of the rock associated with given injection and monitoring intervals.

## 4 Discussion

### 4.1 Comparison with results from steady-state analysis

The inability to analyze many cross-hole tests by means of type-curves led Illman and Neuman [9] to use a steady-state formula developed by Hsieh and Neuman [1] for hydraulic cross-hole tests in saturated rocks. Steady-state analyses are much easier to conduct than transient type-curve [11,6] and numerical inverse [7,8,14] analyses, which have therefore been limited to relatively few single- and cross-hole tests. They found that their steady-state approach performs well for the pressure records, whose signal-to-noise ratio is too low to

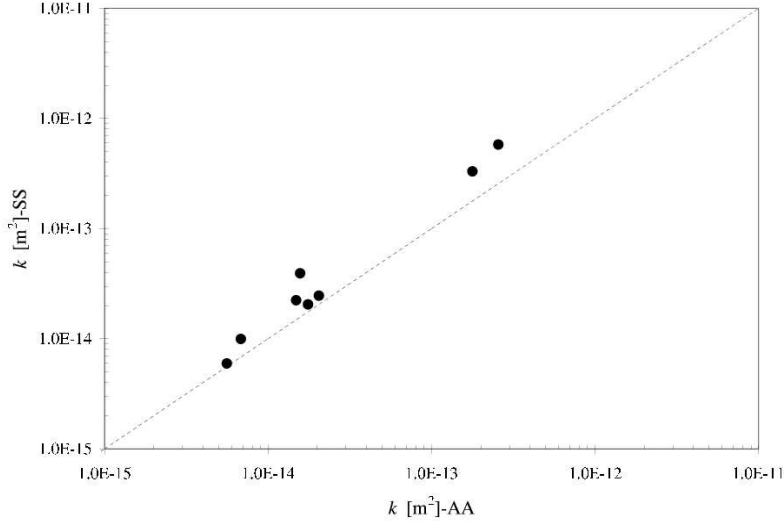


Fig. 5. Comparison of the permeability measurements inferred from the steady-state analysis of Illman [3] and the present transient asymptotic analysis.

allow meaningful transient analysis. They were therefore able to augment in a significant way the database previously established for the ALRS by other means. Though the steady-state method does not yield estimates of porosity, it does yield reliable estimates of permeability between an injection and a monitoring interval. The results were analyzed statistically and they discussed their implications vis-a-vis the pneumatic properties of unsaturated fractured tuff at the ALRS. Their results strengthened the evidence for a previously surmised permeability scale effect at the site.

The results are compared against permeability estimates from the steady-state analysis [3]. Figure 5 shows this comparison revealing that the comparison is quite good with a slight bias toward the steady-state estimates of permeability. This may be due to the fact that the steady-state estimates reflect a larger volume of the rock as the estimates are based on late data. Such a time dependence of permeability was observed in the analysis of pumping test data in fractured carbonates [15].

#### 4.2 Correlation between permeability and porosity

Vesselinov et al. [7,8] developed a three-dimensional numerical inverse model to analyze 5 of the 44 cross-hole tests conducted at the ALRS (i.e., tests PP4 through PP8). The model simulates airflow on a three-dimensional grid of structured and unstructured tetrahedral elements, which represents quite accurately the geometry of vertical and inclined boreholes at the ALRS. Boreholes are treated in the model as high-permeability and high-porosity cylinders of finite length and radius. The model treats permeabilities and porosities ei-

ther as uniform throughout the rock volume or as random fractal fields. In the first case, the estimated parameters represent equivalent values over rock volumes having length-scales ranging from meters to tens of meters, represented nominally by radius vectors extending from the injection interval to the various monitoring intervals. In the second case, they describe the spatial variation of local pneumatic properties throughout the tested rock volume. In their model, this spatial variability was characterized by a power variogram and was estimated geostatistically by Kriging, on the basis of discrete pilot points. Such estimation entailed the simultaneous inversion of pressure records from multiple observation intervals and cross-hole tests. It thus amounts to relatively high-resolution pneumatic tomography, or stochastic imaging, of the rock.

Vesselinov et al. [7,8] analyzed the data first one pressure record at a time making it analogous to the analytical interpretive techniques described here. They noted that each such numerical inversion required  $\approx 80$  forward simulations and it took  $\approx 4$  hours on the University of Arizona SGI Origin multiprocessor supercomputer. To interpret the cross-hole tests with the inverse model, Vesselinov et al. [7,8] filtered the available pressure records so as to focus on signals that appear to be due primarily to air injection and to reduce the large set of recorded pressures done to a manageable number without the significant loss of information. They did so by ignoring those portions of a pressure record that they deemed strongly influenced by barometric pressure fluctuations or other extraneous phenomena and by representing the remaining portions via a relatively small number of “match points.” The match points are distributed more or less evenly along the log-transformed time axis so as to capture with equal fidelity both rapid pressure transients at early time and more gradual pressure variations at later time. Matching was done with equal weighting using the match points with the numerical inverse interpretation.

Vesselinov et al. [8] plotted Kriged and pilot point estimates of  $\log_{10} \phi$  obtained from test PP4 against corresponding estimates of  $\log_{10} k$  and fitted a straight line to these data by regression. They found low correlation coefficients  $r^2$  equal to 0.428 and 0.463 for Kriged and pilot point estimates, respectively. Their hypothesis that the observed scatter can be explained by a linear trend was rejected by a standard Fisher test. The weak linear correlation may be due in part to the effect of correlated estimation errors on the scatter.

The slope of the regression line is  $0.522 \pm 0.004$  for Kriged estimates and  $0.247 \pm 0.174$  for the pilot point estimates. This is equivalent to a 1:2 linear relationship between  $\log_{10} \phi$  and  $\log_{10} k$  based on Kriged estimates and a 1:4 linear relationship based on the pilot point estimates. These authors found it of interest to note that upon reinterpreting data from field conservative tracer tests conducted in saturated fractured rocks on various sites worldwide by different research groups, Guimera and Carrera [16] obtained slopes equal to

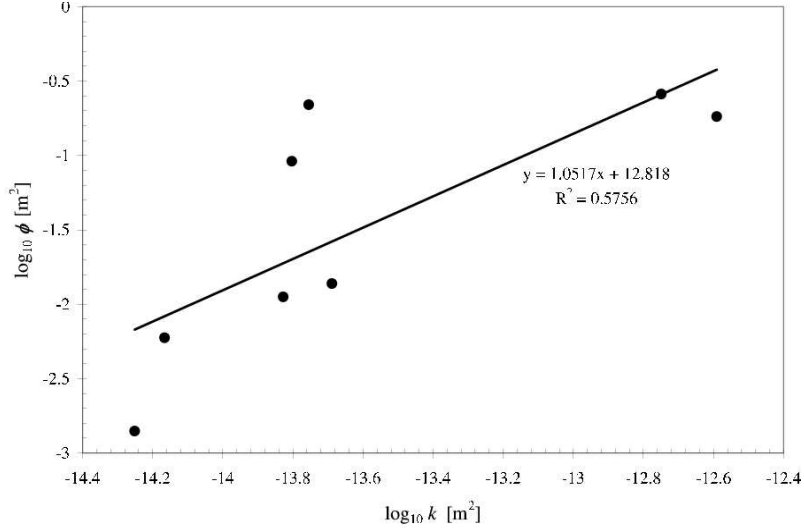


Fig. 6. Correlation between log permeability  $\log_{10} k$  and log porosity  $\log_{10} \phi$ .

0.28 and 0.35 for regression lines of log effective porosity versus log permeability. These are roughly equivalent to a 1:3 linear relationship between the two parameters.

Analysis of the data obtained from the asymptotic analysis of cross-hole test LL2 yielded a slightly higher  $r^2$  equal to 0.576 with a slope of the regression line of 1.052 which is equivalent to a 1:1 linear relationship between  $\log_{10} \phi$  and  $\log_{10} k$  (Figure 6). We attribute the lack of correspondence between the slopes of the regression line obtained here and those obtained by Vesselinov et al. [8] to the differences in the method of interpretation. That is, we treated to the rock to be uniform while Vesselinov et al. [8] treated the rock to be nonuniform described by a power variogram that is characteristic of a random fractal. It is also possible that the differences in the slope is a result of the interpretation of different tests (PP4-PP8 vs LL2) although all the tests were conducted at the same site.

#### 4.3 Scale effects in permeability and porosity

Analyses of single- and cross-hole pneumatic injection tests to date [6,9,7,8] show that the permeability scale effect results from the comparison of single- and cross-hole test data and this can be explained theoretically by treating the permeability field as a self-affine random fractal [17]. However, Illman [3] noted that there is considerable uncertainty whether the comparison of the data from the two types of tests really reveal a scale effect because the tests were conducted in a different configuration that could potentially introduce an experimental bias.

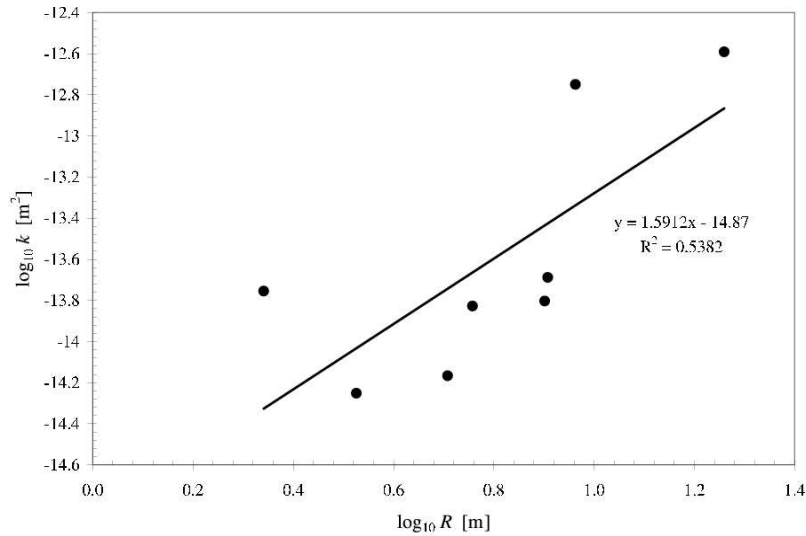


Fig. 7. Log permeability  $\log_{10} k$  as a function of  $\log_{10} R$ .

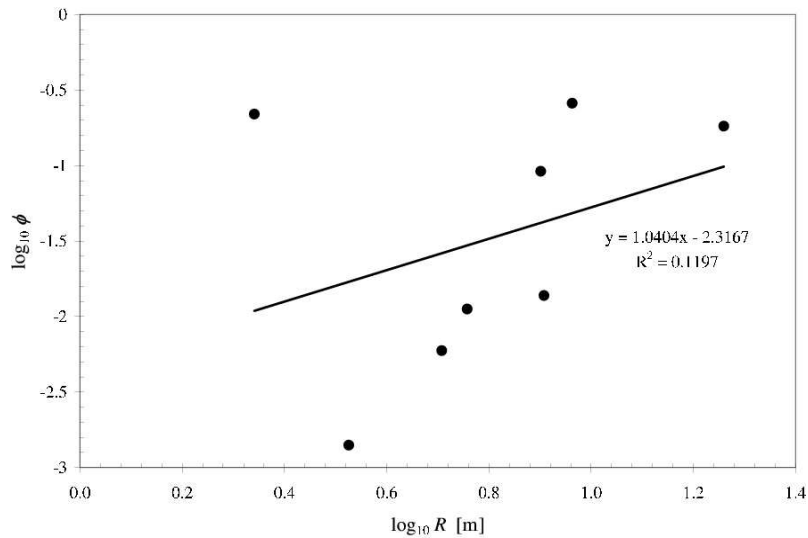


Fig. 8. Log porosity  $\log_{10} \phi$  as a function of  $\log_{10} R$ .

The single-hole tests were conducted along the boreholes in 11 boreholes where the bulk of the rock is unfractured and so they will be representative of the combined properties of the fracture and rock matrix. Fracture porosity determined from cross-hole tests range between  $10^{-4}$  to  $10^{-2}$  suggesting that only a small portion of the rock conducts flow. Therefore, Illman [2004, submitted manuscript] reasoned that a “true” scale effect can only be measured from the comparison of permeabilities from a single type of test conducted over a large range of scales at various configurations. As the cross-hole tests at the ALRS were conducted in a tomographic manner with air injection taking place from different directions while corresponding monitoring interval pressures were monitored in all neighboring intervals. These attributes of the cross-hole tests show that cross-hole tests at the ALRS may be able to measure a “true” scale effect. Using the steady-state solution [1], Illman [3] showed a strong field ev-

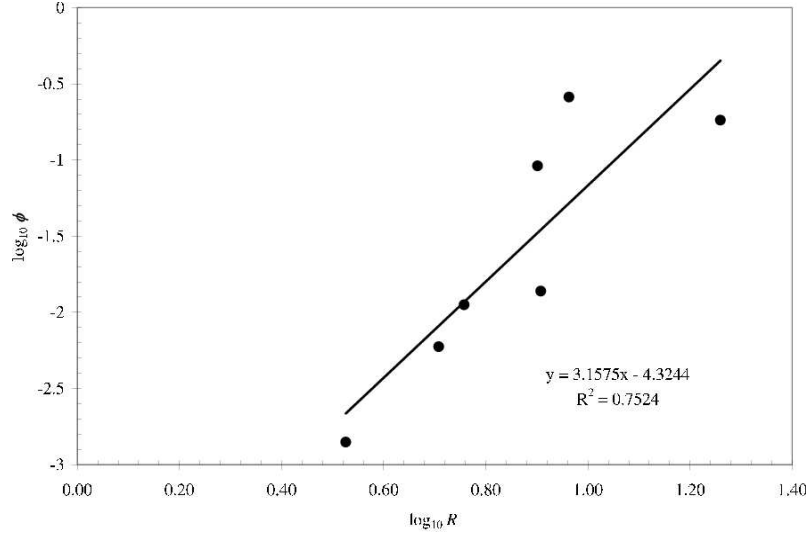


Fig. 9. Log porosity  $\log_{10} \phi$  as a function of  $\log_{10} R$  with V2 data treated as an outlier.

idence for a permeability scale effect from cross-hole tests alone by plotting the calculated permeabilities against the radial distance between the injection intervals. As he used a steady-state equation to analyze the data, he was only able to obtain estimates of permeability only from the various tests that he analyzed. Here, we used the asymptotic approach to obtain the estimates of permeability and porosity showing that both parameters increase with radial distance from the injection interval (Figures 7 and 8), i.e., with the measurement scale. The correlation between porosity scaling is  $\log_{10} R$  and  $\log_{10} \phi$  is very weak because of the strong influence of the high value of porosity in V2 near the injection interval. If we treat this value to be an outlier and replot the graph, we see that the correlation improves dramatically (Figure 9).

## 5 Conclusions

This study leads to the following major conclusions:

- (1) We developed a new method to interpret three-dimensional pressure interference tests based on the asymptotic analysis of late time pressure transient data. The approach yields reliable estimates of equivalent permeability and porosity which can be obtained without the construction of type-curves or numerical inverse models. The approximation presented in [4] is strictly valid for the case when the injection and monitoring intervals can be idealized as points. Here, we extend their analysis by developing an asymptotic solution for the line-injection line-monitoring solution [1] and studying the late-time behavior. A comparison of our asymptotic solution to the original line-injection/line-observation solution [1] reveals

that the approximation is very good at intermediate to late time (small  $t_d^{-1/2}$ ) with the correspondence improving as  $\alpha_1 = \beta_1$  increases. For all practical purposes the approximation can be used when  $\alpha_1 = \beta_1 > 0.2$ . The major advantage of our new approach to existing type-curve methods is that there is not need to plot a type-curve, which can be sometimes difficult to acheive.

- (2) We apply the technique to a cross-hole pneumatic injection test conducted at the Apache Leap Research Site near Superior, Arizona [5,2] and compare these results to previously obtained estimates of permeabilities from steady-state analysis in [3]. The comparisons reveal that the newly developed approach yields reliable estimates of permeabilities and porosities from three-dimensional pressure interference tests.
- (3) The asymptotic analyses are much easier to conduct than transient type-curve [11,6] and numerical inverse [14,7,8] analyses, which have therefore been limited to relatively few single-hole and cross-hole tests. We found our asymptotic approach to work well for pressure records whose signal-to-noise ratio is too low to allow meaningful transient analysis. This also includes cases when pressure transients are heavily affected by borehole storage, external forcings, and heterogeneities that cause the data to depart from analytically derived type-curve models. We were therefore able to augment in a significant way the database previously established for the ALRS by other means. In addition to estimates of permeability, the asymptotic approach yields reliable estimates of porosity between an injection and a monitoring interval, which cannot be obtained from the steady-state analysis of the same data.
- (4) Comparison of permeabilities obtained from the asymptotic to steady state analysis is good although the permeabilities are slightly biased toward higher permeability values for the steady-state approach. This may be due to the fact that the steady state portion of the pressure transient has sampled a larger portion of the rock giving rise to larger equivalent directional permeabilities. We emphasize that the steady-state analysis does not yield estimates of porosity but the asymptotic analysis does.
- (5) Our analysis of pressure transient data assumes that the rock is pneumatically uniform and isotropic on the scale of the cross-hole test. Results from individual monitoring intervals provided information about pneumatic connections between these and the injection interval, corresponding directional permeabilities, and porosities. Each pressure record yielded an equivalent directional permeability and porosity for fractures that connect the corresponding monitoring and injection intervals. Both quantities were found to vary considerably from one pressure monitoring record to another. Thus, even though our asymptotic analysis treats the rock as if it was pneumatically uniform and isotropic, it ultimately yields information about the spatial and directional dependence of pneumatic connectivity, permeability and porosity of fractures across the site on

- scales relevant to the cross-hole test.
- (6) There is a 1:1 linear relationship between our estimates of log porosity and log permeability at ALRS from cross-hole test LL2. This is different from the weak 1:4 to 1:2 linear relationship found in [8]. We attribute the lack of correspondence between the slopes of the regression line obtained here and those obtained in [8] to the differences in the method of interpretation. That is, we treated the rock to be uniform while [8] treated the rock to be nonuniform described by a power variogram that is characteristic of a random fractal. It is also possible that the differences in the slope is a result of the interpretation of different tests (PP4-PP8 vs LL2) although all the tests were conducted at the same site.
  - (7) Analyses of single- and cross-hole pneumatic injection tests to date [9,6–8] show that the permeability scale effect results from the comparison of single- and cross-hole test data and this can be explained theoretically by treating the permeability field as a self-affine random fractal [17]. However, considerable uncertainty remains whether the comparison of the data from the two types of tests really reveal a scale effect because the tests were conducted in a different configuration that could potentially introduce an experimental bias [3]. Here, we used the asymptotic approach and obtain estimates of both permeability and porosity showing that both parameters increase with radial distance from the injection interval which we treat it to be the measurement scale. These results show that the cross-hole test results from test LL2 alone show a scale effect in both parameters. However, the relationship between porosity and scale is very weak.

## 6 Acknowledgements

The first author was supported in part by the 2003 Old Gold Fellowship from the University of Iowa, as well as by funding from the National Science Foundation (NSF) and the Strategic Environmental Research & Development Program (SERDP). The research by the second author was performed at Los Alamos National Laboratory under the auspices of the U.S. Department of Energy, contract W-7405-ENG-36; and was supported by the LDRD Program at Los Alamos National Laboratory.

## References

- [1] P. A. Hsieh, S. P. Neuman, Field determination of the three-dimensional hydraulic conductivity tensor of anisotropic media, 1. Theory, *Water Resour. Res.* 21 (11) (1985) 1655 – 1665.

- [2] W. A. Illman, D. L. Thompson, V. V. Vesselinov, G. Chen, S. P. Neuman, Single- and cross-hole pneumatic tests in unsaturated fractured tuffs at the apache leap research site: Phenomenology, spatial variability, connectivity and scale, Tech. Rep. NUREG/CR-5559, U. S. Nucl. Regul. Comm., Washington D.C. (1998).
- [3] W. A. Illman, Strong field evidence of permeability scale effect in fractured rock, Submitted manuscript .
- [4] W. A. Illman, D. M. Tartakovsky, Asymptotic analysis of three-dimensional pressure interference tests: Point source solution, Water Resour. Res. Submitted manuscript.
- [5] W. A. Illman, Single- and cross-hole pneumatic injection tests in unsaturated fractured tuffs at the Apache Leap Research Site near Superior, Arizona, Ph.D. thesis, Dep. of Hydrol. and Water Resour., University of Arizona, Tucson (1999).
- [6] W. A. Illman, S. P. Neuman, Type-curve interpretation of a cross-hole pneumatic test in unsaturated fractured tuff, Water Resour. Res. 37 (3) (2001) 583 – 604.
- [7] V. V. Vesselinov, S. P. Neuman, W. A. Illman, Three-dimensional numerical inversion of pneumatic cross-hole tests in unsaturated fractured tuff: 1. Methodology and borehole effects, Water Resour. Res. 37 (12) (2001) 3001 – 3017.
- [8] V. V. Vesselinov, S. P. Neuman, W. A. Illman, Three-dimensional numerical inversion of pneumatic cross-hole tests in unsaturated fractured tuff: 2. Equivalent parameters, high-resolution stochastic imaging and scale effects, Water Resour. Res. 37 (12) (2001) 3019 – 3041.
- [9] W. A. Illman, S. P. Neuman, Steady-state analyses of cross-hole pneumatic injection tests in unsaturated fractured tuff, J. Hydrol. 281 (2003) 36 – 54.
- [10] H. H. C. Jr., C. E. Jacob, A generalized graphical method for evaluating formation constants and summarizing well field history, EOS Transactions 27 (1946) 526 – 534.
- [11] W. A. Illman, S. P. Neuman, Type-curve interpretation of multi-rate single-hole pneumatic injection tests in unsaturated fractured rock, Ground Water 38 (6) (2000) 899 – 911.
- [12] T. C. Rasmussen, D. D. Evans, P. J. Sheets, J. H. Blanford, Unsaturated fractured rock characterization methods and data sets at the Apache Leap tuff site, Tech. Rep. NUREG/CR-5596, U. S. Nucl. Regul. Comm., Washington D.C. (1990).
- [13] A. G. Guzman, A. M. Geddis, M. J. Henrich, C. F. Lohrstorfer, S. P. Neuman, Summary of air permeability data from single-hole injection tests in unsaturated fractured tuffs at the Apache Leap Research Site: Results of steady-state test interpretation, Tech. Rep. NUREG/CR-6360, U. S. Nucl. Regul. Comm., Washington D.C. (1996).

- [14] V. V. Vesselinov, S. P. Neuman, Numerical inverse interpretation of single-hole pneumatic tests in unsaturated fractured tuff, *Ground Water* 39 (5) (2001) 685 – 695.
- [15] D. Schulze-Makuch, D. S. Cherkauer, Variations in hydraulic conductivity with scale of measurement during aquifer tests in heterogeneous, porous carbonate rocks, *Hydrogeology J.* 6 (1998) 204 – 215.
- [16] J. Guimera, J. Carrera, A comparison of hydraulic and transport parameters measured in low permeability fractured media, *J. Cont. Hydrol.* 41 (2000) 261 – 281.
- [17] Y. Hyun, S. P. Neuman, V. V. Vesselinov, W. A. Illman, D. M. Tartakovsky, V. D. Federico, Theoretical interpretation of a pronounced permeability scale effect in unsaturated fractured tuff, *Water Resour. Res.* 38 (6) (2002) doi:10.1029/2001WR000658.